Biomedical Signal Processing and Control 7 (2012) 419–428

Contents lists available at SciVerse ScienceDirect

Biomedical Signal Processing and Control

journal homepage: www.elsevier.com/locate/bspc

Review

Ultrasound image enhancement: A review

Sonia H. Contreras Ortiz[a,b,*], Tsuicheng Chiu[a], Martin D. Fox[a]

[a] Department of Electrical and Computer Engineering, Biomedical Engineering Program, University of Connecticut, 260 Glenbrook Rd., Storrs, CT 06269-2247, USA
[b] Electronic Engineering Program, Universidad Tecnológica de Bolívar, Parque Industrial y Tecnológico Carlos Vélez Pombo, Km 1 Vía Turbaco, Cartagena de Indias, Colombia

ARTICLE INFO

Article history:
Received 28 June 2011
Received in revised form 4 February 2012
Accepted 21 February 2012
Available online 17 March 2012

Keywords:
Ultrasound imaging
Ultrasound enhancement
Speckle reduction

ABSTRACT

Medical ultrasound imaging uses pulsed acoustic waves that are transmitted and received by a hand-held transducer. This is a mature technology that it is widely used around the world. Among its advantages are that it is cost-effective, flexible, and does not require ionizing radiation. However, the image quality is affected by degradation of ultrasound signals when propagating through biological tissues. Many efforts have been done in the last three decades to improve the quality of the images. This paper reviews some of the most important methods for ultrasound enhancement. We classified these techniques into two groups: preprocessing and post-processing, analyzed their benefits and limitations, and presented our beliefs about where ultrasound research could be directed to, in order to improve its effectiveness and broaden its applications.

Contents

* Corresponding author at: Department of Electrical and Computer Engineering, Biomedical Engineering Program, University of Connecticut, 260 Glenbrook Rd., Storrs, CT 06269-2247, USA.
E-mail addresses: scontreras@unitecnologica.edu.co, soniahcon@gmail.com (S.H. Contreras Ortiz), tsui-cheng.chiu@uconn.edu (T. Chiu), fox@engr.uconn.edu (M.D. Fox).

1746-8094/$ – see front matter © 2012 Elsevier Ltd. All rights reserved.
doi:10.1016/j.bspc.2012.02.002

1. Introduction

Ultrasound is a widely used medical imaging modality. Key applications include cardiology, urology, obstetrics and gynecology, general abdominal imaging, vascular imaging, and it can be used as a guide in surgical procedures. Outside the United States, and especially in developing countries, ultrasound is the most common diagnostic imaging technique after radiography. In the United States, ultrasound is broadly used by physicians although radiologists often prefer other high technology modalities such as computed tomography (CT) and magnetic resonance imaging (MRI) [1,2].

Commercially available ultrasound scanners generate the images under the principle of echo imaging. Pulsed acoustic waves with frequencies ranging from 1 to 20 MHz are transmitted into the body using a hand-held transducer. After interacting with tissues, some of the transmitted energy returns to the transducer to be detected by the instrument. The principles of echo localization were first applied for medical purposes in the early 1950s and advances in technology in the last decades have increased the usefulness of ultrasound. Some of the advantages of ultrasound are:

- It is inexpensive compared to other modalities such as CT and MRI.
- It is compact and portable.
- It works in real-time.
- The transducer is small and easily manipulable.
- It is noninvasive.
- It does not require ionizing radiation.

The main drawback of ultrasound is its limited penetration. Sound waves cannot pass through bone or air, and this restricts the use of ultrasound in the brain, lungs and the abdominal region. In addition to that, it is very difficult to obtain diagnostic images on patients that are overweight. Other limitation of ultrasound is that its usefulness depends on the skill of the technician or physician performing the examination. As ultrasound images are not complete tomographic slices, lack of context make them harder to read, and the results are often difficult to reproduce. In other technologies such as CT and MRI, the slice axes are typically generated perpendicular to the longitudinal axis of the body, so they can be considered more objective and reproducible [1].

Image quality is a key aspect to consider, and the focus of this paper. Ultrasound images are affected by many types of artifacts, making it hard for an observer to interpret the images and obtain quantitative information from them. Despite of the limitations of ultrasound, it is still the most safe and cost-effective imaging modality in many applications, so many efforts have been done to make the images more valuable. The purpose of this paper is to provide an overview of the techniques for ultrasound image enhancement.

Ultrasound enhancement methods can be classified in two main groups: preprocessing and post-processing techniques. Preprocessing techniques deal with image degradation related to the physical properties of the signals involved (coherence, bandwidth, nonlinear propagation, attenuation, absorption, etc.), and consist of modifications in the signal generation and/or image acquisition stages. Examples of this category include spatial and frequency compounding, harmonic imaging, and pulse inversion. Post-processing algorithms, on the other hand, use signal processing techniques to enhance the images after they have been captured. Filtering and deconvolution are two examples of these techniques.

It is important to mention that the foundation of image quality improvement is on the evolution of the technology of ultrasound scanners: transducer materials and construction, electronics for signal generation, acquisition and visualization, computational capability and digital processing, etc. These topics were not included in this review, but further information can be found in [3–5]. The rest of the paper is organized as follows: Section 2 discusses the image formation and the main artifacts that affect its quality. Sections 3 and 4 review some of the most common preprocessing and post-processing enhancement techniques, and Section 5 concludes the paper.

2. Background

2.1. Image formation

Ultrasound provides a noninvasive technique for imaging human anatomy. In medical ultrasound, a pulsed wave $p(t)$ excites a piezoelectric transducer and an acoustic wave is sent through the patient's body. When the wavefront hits a discontinuity, scattered waves are produced. These echoes are detected by the same transducer, processed and displayed. If tissues are modeled as arrays of isotropic scatterers having a reflectivity $R(x, y, z)$, and for ultrasound waves propagating in the z direction, the resultant processed signal $e(t)$ can be written [6]

$$e(t) = K\left|\int\int\int \frac{e^{-2\alpha z}}{z} R(x,y,z)\, s(x,y)\, \tilde{p}\left(t - \frac{2z}{c}\right) dx\, dy\, dz\right| \quad (1)$$

where K is a normalizing constant, $e^{-2\alpha z}$ is the attenuation in the tissue through the roundtrip distance of $2z$, $s(x, y)$ is the transducer field pattern, and $\tilde{p}(t - 2z/c)$ is the received pulse delayed by the roundtrip time $2z/c$. It is assumed that the extent of the transducer's face is very large compared to the wavelength of the propagating wave, and $s(x, y)$ is constant over the transducer face and zero elsewhere. Thus, $\tilde{p}(t)$ is the convolution of the transmitted pulse $p(t)$ with the impulse responses of the transducer and the filters in the processor. The absolute value in Eq. (1) represents the envelope detection, and the factor $1/z$ is the loss of amplitude due to diffraction spreading from each scatterer. The signal processor includes a system of time-varying gain to compensate for attenuation, therefore, Eq. (1) can be simplified as follows

$$e_c(t) = K\left|\int\int\int R(x,y,z)\, s(x,y)\, \tilde{p}_e\left(t - \frac{2z}{c}\right) e^{j2\pi f_0(2z/c)}\, dx\, dy\, dz\right| \quad (2)$$

In Eq. (2), the pulse was expressed as the product of an envelope function and a radio frequency (RF) signal with center frequency f_0. The signal $e_c(t)$ is called the A-mode signal and it is used directly in the formation of B-mode images. Commercially available ultrasound scanners do not typically display the true amplitude of the envelope signal because of its large dynamic range. The signal is

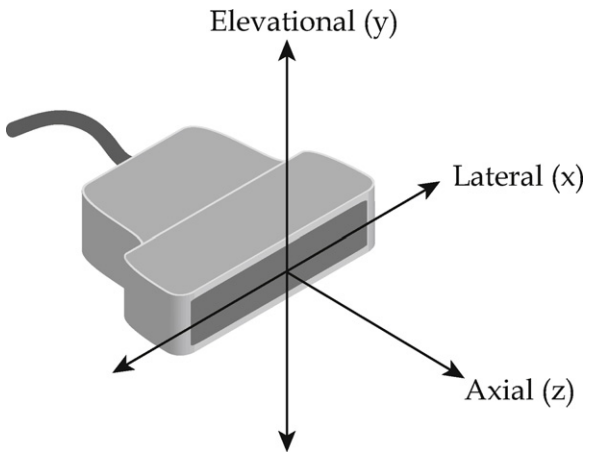

Fig. 1. An ultrasound transducer and the three directions that define ultrasound resolution.

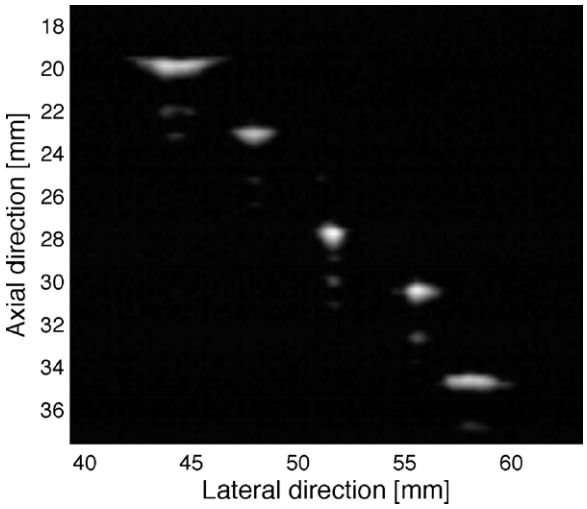

Fig. 2. Variability of the PSF in the axial direction. To simulate point targets, a wire phantom was built using 0.1 mm diameter nylon thread. The image was acquired with the GE RT 3200 scanner (GE Healthcare, Milwaukee, WI) using a 7.5 MHz linear transducer. The transducer is located in the top of the image, and the focal distance is 27 mm.

logarithmically compressed before being displayed, and this process can be modeled as follows

$$X = D\ln(A) + G \tag{3}$$

where A is the detected A-mode signal, D is related to the dynamic range of the input and G to the gain of the compressor. The signal $e_c(t)$ can be thought of as an estimate of the reflectivity function as a function of spatial location [7]

$$\hat{R}(x,y,z) = e_c\left(\frac{2z}{c}; x, y\right) \tag{4}$$

Therefore, the resulting expression for the reflectivity using convolutional form is

$$\hat{R}(x,y,z) = K\left|R(x,y,z)\,e^{j2kz} * s(-x,-y)\,\tilde{p}_e\left(\frac{2z}{c}\right)\right| \tag{5}$$

where $k = 2\pi f_0/c$.

2.2. Point spread function (PSF)

The PSF of an imaging device is the response of the system to an ideal point target. It is a 3D shape and is also known as the resolution cell of the system. The PSF is caused by diffraction spreading of the ultrasound signals that results in blurred images. The resolution in ultrasound can be analyzed using Eq. (5). If the exponential term is ignored, the estimated reflectivity can be modeled as the true reflectivity convolved with the PSF, given by the product of the transducer field shape and the pulse [7].

Fig. 1 shows the diagram of a transducer and the three directions used to define ultrasound resolution. The axial direction is the direction of propagation of the sound waves. The lateral and elevational (out of plane) directions are associated to the width and height of the transducer's face respectively.

Ultrasound resolution is not isotropic. Axial resolution is approximately half the pulse length, and is relatively constant with depth. On the other hand, lateral resolution is equal to the beam width in the image plane and varies with depth being optimum in the focal region of the transducer. As the shape of the PSF depends on the reflector's distance to the focus, the imaging system is shift variant along the axial direction but shift invariant along the lateral and elevational directions [8]. This lateral and elevational shift invariance only holds when scanning in a rectilinear fashion and under the assumption of weak scattering. Fig. 2 shows the variation of the PSF in the axial direction. As the pulse width is generally larger than the pulse length, axial resolution is better than lateral resolution. The transmit-receive aperture width is much smaller in the elevational direction than in the lateral direction. Consequently, resolution in the elevational direction is the worst and the PSF has sidelobes of higher amplitude [8].

2.3. Artifacts of ultrasound images

Ultrasound images have in general low signal to noise ratio (SNR) and there are three main reasons for that. First, ultrasound scanners use pulsed signals that have short duration in time and therefore a broad spectrum in frequency domain. As a result, the signals can be affected by multiple noise sources. Second, the coherent nature of the signals gives rise to speckle noise. And third, sound waves are highly distorted when traveling through the tissues. Consequently, ultrasound images have many types of artifacts that affect their quality. Examples of artifacts are presented in Figs. 3 and 4. These images were acquired with the GE RT 3200 scanner using a 7.5 MHz linear transducer. Fig. 3 shows the image of a breast phantom (Model BB-1, ATS laboratories, Bridgeport, CT) within a water tank, and Fig. 4 shows the image of a hypo-echoic mass in a contrast phantom (Model 531, ATS laboratories, Bridgeport, CT), and the image of a metallic pin within a water tank. The artifacts observed in these images distort the shape and texture of the structures and obscure their details. Below there is a description of the most common ultrasound artifacts. We have classified them into three groups: wave propagation artifacts, attenuation artifacts and speed of sound artifacts.

2.3.1. Wave propagation artifacts

Speckle

Speckle occurs when scanning targets below the pulse resolution, and results from the accumulation of independently-phased wavefronts. This phenomena can be described geometrically as a random walk of component phasors [9,10]. Scattering from targets within the resolution cell undergo constructive and destructive interference that results in intensity fluctuations in the image, and degrades its quality (Fig. 3). Speckle is represented by the exponential term in Eq. (5) [7].

The statistics of speckle vary according to the physical properties of the structures being imaged. When there is a large number of scatterers within the resolution cell ($N_s > 10$), it can be assumed, under the central limit theorem, that the real and imaginary components of the phasors are normally distributed. Therefore, the magnitude of the scattered field follows the Rayleigh probability

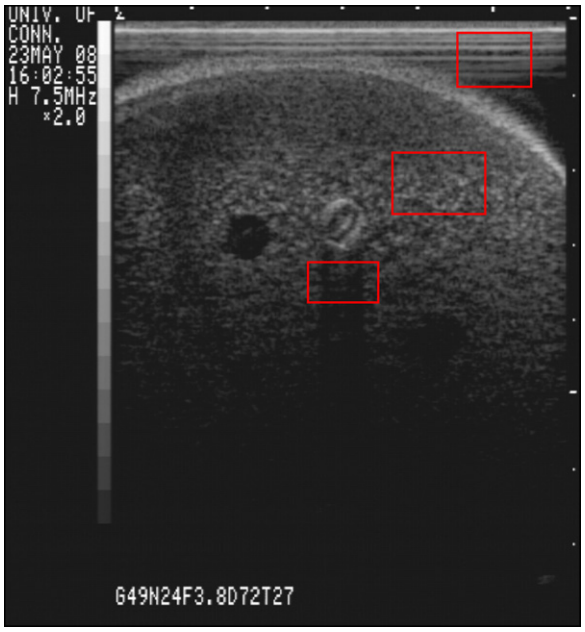

Fig. 3. Image of a breast phantom where several artifacts are apparent. The enclosed regions show examples of artifacts. Top: reververations. Middle: speckle. Bottom: shadowing.

density function and the phase is uniformly distributed between 0 and 2π [11]. This is the case of fully developed speckle and has a constant SNR equal to 1.92. Partially and fully structured regions have different speckle patterns that have been modeled with the Rician and K-distributions [10,12]. Logarithmic compression changes the statistics of speckle, so previous works have used the extreme value distribution [13], and the Gaussian distribution [14] to model speckle in logarithmically compressed images.

Reverberations

Reverberations are multiple reflections that occur when two or more reflectors are located in the sound path [15]. Reverberations are seen as additional parallel bright lines with separation equal to the separation of the real reflectors (Fig. 3).

Comet tail

Certain reflectors produce series of closely spaced discrete echoes. This artifact is known as comet tail and it is a form of reverberation. Later echoes may have decreased amplitude due to attenuation, and this reduction in amplitude is displayed as a decreased width [16] (Fig. 4).

Ring down

The ring down artifact occurs when short-range reverberations are resonant. Discrete echoes cannot be identified because they are too close together. As a result, a continuous sound wave is transmitted back to the transducer [15].

Side lobes

Side lobes consist of multiple sound beams of less intensity that occur outside the main beam. They can create detectable echoes from strong reflectors situated off the central axis of the main beam [17] (Fig. 4).

Mirror image

In presence of a strong reflective interface, sound waves bounce off the reflector, and then, in presence of an structure, bounce back to the reflector before returning to the transducer to be detected. The scanner assumes a straight line path of the signal and places a duplicate of the structures behind the reflector [15,16].

2.3.2. Attenuation artifacts

Acoustic shadowing

Acoustic shadowing is the reduced intensity of echoes caused by intervening structures with high attenuation (Fig. 3). When an object is shown brightly, it indicates strong reflection and likely high absorption. Therefore, the sound waves passing through it turn to be weaker. This results in dark presentation of tissues distal to the object [15]. Shadowing is commonly seen in bones and all types of calcifications, and where there is a large impedance mismatch between two tissues, such as gas and soft tissues.

Enhancement

In the focal region there is an increased intensity of the ultrasound signal, and the structures appear brighter. This artifact is known as focal enhancement, and is shown in Fig. 4. Distal enhancement, on the other hand, is the relative increase of echoes caused by an intervening structure of low attenuation, i.e. the scanner assumes that the attenuation in the propagation path is higher than it really is [15].

2.3.3. Speed of sound artifacts

Speed of sound errors

Ultrasound scanners assume a constant value for the speed of sound in tissues ($1540\,m/s$) to generate the B-mode images. Therefore, changes in speed of sound inside the tissues distort the appearance, shape and size of the structures being imaged [15].

Refraction

Refraction occurs when there is a change in direction of the ultrasound beam as it crosses a boundary of two regions with different speed of sound. It can cause errors in the lateral positioning of the structures [15].

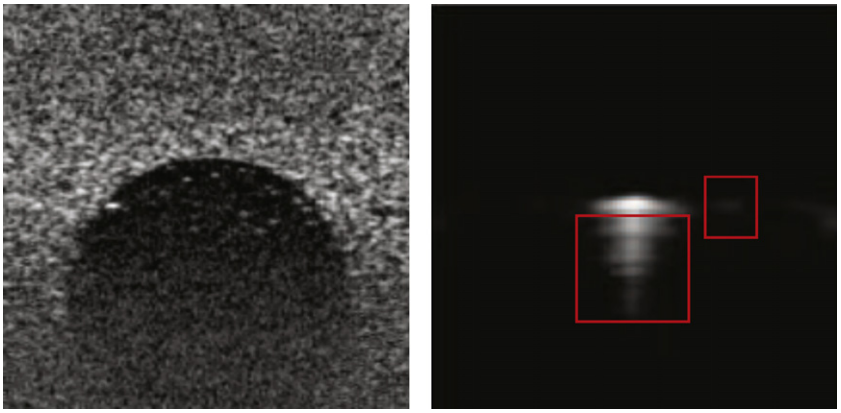

Fig. 4. Left: image of a hypo-echoic mass in a contrast phantom. The focal region has increased brightness and contrast. Right: image of a metallic pin within a water tank. The comet tail and side lobe artifacts can be seen inside the rectangles. The comet tail appears below the pin and the side lobe on the right.

3. Preprocessing enhancement techniques

Preprocessing techniques attempt to shape the ultrasound field to compensate for known degradations due to tissue properties. They consist of modifications in the signal generation and/or acquisition stages. Examples of these techniques include modern beamforming, compounding, harmonic imaging, and pulse inversion. The purpose of modern beamforming techniques is to model the ultrasound beam for improved propagation in order to reduce artifacts, and overcome trade-offs such as resolution/penetration, and contrast/resolution. Compounding combines multiple images to produce a higher quality image. Harmonic imaging and pulse inversion are two techniques that were developed for contrast imaging. Harmonic imaging refers to the use of the harmonic components that are generated when the sound waves travel through the tissues. Pulse inversion, on the other hand, analyzes the differences between two received echoes resulting from the consecutive transmission of an ultrasound wave and its inverted replica.

3.1. Modern beamforming techniques

Beamforming techniques have evolved to generate ultrasound beams whose propagation is less affected by tissue inhomogeneities. They can reduce artifacts such as side-lobes and speed of sound errors, and can improve penetration without sacrificing resolution. Examples of modern beamforming techniques include dynamically focused transmission and reception, apodization, limited diffraction beams, and pulse compression.

3.1.1. Dynamically focused transmission and reception

Dynamically focused reception consists of sweeping the focus of an array transducer along the beam by changing the time delays associated with the active transducer elements, so that echoes from all depths are always in focus. This technique allows an increased depth of field without reducing lateral resolution [18]. The change of focal length can be done electronically in real-time, so the frame rate is not affected. Dynamically focused transmission, on the other hand, constructs the image with a montage process, where images obtained with different transmission focal lengths are cut around the focus and mounted together. In this case the frame rate is reduced. Dynamic focusing in both transmission and reception allows improved lateral resolution and reduced side lobes [18]. A different approach called synthetic aperture was proposed by Jensen et al. [19]. In this method, a set of low resolution images are created by exciting a single element in the transducer at a time and acquiring the echoes from all elements. Focusing is performed in reception and a high resolution image is reconstructed by combining the low resolution images. The results show improved contrast, resolution and depth of field.

3.1.2. Apodization

The weights of individual samples in finite duration signals can be adjusted to obtain desirable characteristics in frequency domain such as a narrow main lobe and reduced side lobes. This is a classic problem in signal processing for the design of finite impulse response (FIR) filters. Ultrasound scanners use aperture weighing functions to improve resolution and reduce side lobes, and this technique is called apodization. Some works on ultrasound apodization are mentioned next. Mandersson and Salomonsson [20] proposed a weighted least-squares filter to decrease the duration of ultrasound echoes with the purpose of increasing resolution. Wilkening et al. [21] designed optimal FIR filters to improve contrast in contrast agent imaging. Finally, Guenther and Walker [22] used constrained least-squares techniques to describe the system PSF as a function of the aperture weightings. This method can achieve optimal contrast by designing mathematically optimal aperture weights for a given system.

3.1.3. Limited diffraction beams

Limited diffraction beams are solutions to the wave equation that produce beams with a large depth of field and an approximate depth-independence property. Examples of limited diffraction beams are the Bessel beams and the X waves [18]. The downside of these beams is that they produce very large side lobes, what can reduce image contrast.

3.1.4. Pulse compression

Ultrasound imaging traditionally involves the transmission of a brief pulse with a constant central frequency, what results in a trade-off between resolution and penetration. Pulse compression is a different approach where the transmitted pulse has longer duration and lower amplitude than the traditional pulse, and its frequency is either swept so that it is a chirp, or it is modulated using linear on nonlinear frequency modulation (FM), or a binary code. Pulse compression increases SNR by selecting appropriate coding, what results in improved penetration with good resolution. The decoding filter compresses the code energy into a short time interval, and it is usually implemented with a matched filter, for optimal detection SNR [23–26].

3.2. Compounding

Compounding is an approach that combines images acquired from different angles or aperture positions, or using multiple frequencies, with the purpose of reducing artifacts and improving resolution. Speckle is averaged out when images that have uncorrelated or partially correlated speckle patterns are combined. If N images are used in the reconstruction, the reduction in speckle is of the order of $\sqrt{N}$ when the images are statistically independent [11]. Fig. 5 shows the simulated image of a cyst phantom obtained with the software Field II [27,28], and the resultant image after averaging 10 independent images [29]. SNR in the background was improved about 3 times, what is closed to the maximum expected improvement when combining 10 independent images ($\sqrt{10} = 3.16$). The improvement in SNR is lower than $\sqrt{N}$ when the images are correlated [30]. However, some works have demonstrated that by using weighted averaging, it is possible to get the maximum improvement with partially correlated images [31,32].

Resolution can be improved by compounding because by combining images taken from different angles, the PSF becomes more isotropic and uniform across the image. With respect to artifacts, shadowing can be reduced because structures that are obscured by high reflectors appear when the ultrasound beam comes from a different direction. There are three main types of compounding: spatial compounding, frequency compounding and strain compounding. Below there is an explanation of each technique.

3.2.1. Spatial compounding

There are several approaches for spatial compounding. The ultrasound beam can be electronically steered to several angles and the images taken from these angles are then combined [33,34]. The transducer or the sample can be rotated to acquire the images from multiple angles, and they are registered (aligned) before compounded. The images can also be acquired by displacing the transducer laterally [35,29] or using a combination of lateral and angular displacements [36].

Bashford and Morse [32], Hansen et al. [37] and Macione et al. [38] developed custom designed mechanical systems to rotate the transducer and acquire the images. These systems hold the transducer in one horizontal plane and rotate it 360° around the sample.

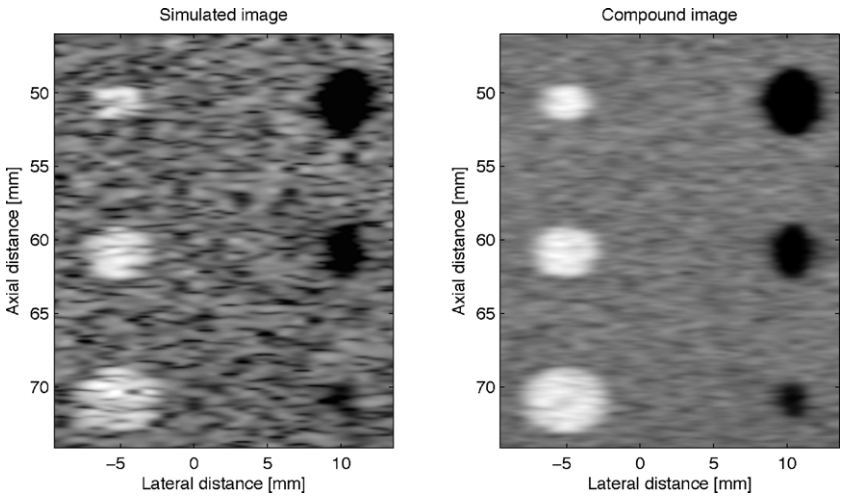

Fig. 5. Illustration of the improvement of SNR by compounding. Left: simulated image of a cyst phantom. Right: compound image using 10 independent images. The images were generated using 100,000 point scatterers randomly distributed within the field.

Spatial compounding can also be applied in the elevational direction. If a 2D array is available, partially correlated measurements can be obtained by steering the image plane elevationally with small inclinations as proposed by Pai Chi and ODonnell [39]. The main drawback of these techniques is the reduction in the frame rate due to the need for multiple images. A solution to this problem was proposed by Behar et al. [40]. They developed a system with three transducers: a central transducer that performs as transmitter and receiver and two lateral unfocused piston transducers that perform only as receivers. This system allows spatial compounding without reducing the frame rate. A later publication of this group [41] uses filtering on the compound images to further improve their quality.

Even though the most common method of combining the images is averaging, there are other operators that have been studied. Wilhjelm et al. [42] analyzed the results of compounding images using six different operators: mean, median, mean excluding maximum (mem), root mean square (rms), geometric mean (geomean) and maximum. The results show that for the mean operator, the SNR and contrast increased with increasing number of images. The rms and geomean operators showed reduced improvement in SNR and contrast, relative to the mean operator. The median and mem provided differently looking images and good improvements in SNR and contrast. Finally, Macione et al. [38] proposed a nonlinear compound technique that consists on the multiplication of pairs of component images followed by the summation of products.

3.2.2. Frequency compounding

Frequency compounding combines images acquired using multiple frequencies. It can be applied on transmit mode by using multiple sources at different frequencies [43–46] or on receive mode by dividing the spectrum of the RF echoes into sub-bands to make separate images [47,48]. Early works on frequency compounding noticed that when having a fixed bandwidth system, the reduction in speckle was at the price of axial resolution and overall image quality [44]. Recent works have tried to overcome this limitation by increasing the effective bandwidth of the system. Dantas and Costa [48] proposed a bank of wideband 2D directive filters, based on modified Gabor functions. Each filter is applied to the 2D RF data. By compounding the filters' outputs, speckle is reduced and the structure information is enhanced. Sanchez et al. [49] proposed a combination of frequency compounding with the coded excitation and pulse-compression technique called resolution enhancement compression (REC). Using REC the bandwidth and axial resolution of the system was doubled and frequency compounding used this larger available bandwidth to improve image contrast. Chang et al. [46] used a concentric annular type high-frequency dual element transducer to broaden the bandwidth. The transducer elements operated at 20 and 40-MHz and the results showed that the image SNR could be increased with a small reduction in axial resolution.

3.2.3. Strain compounding

Strain compounding was proposed by Li and Chen [50]. In this approach different strain states are created using external forces that produce three dimensional tissue motion. If only lateral and axial movements are corrected, the images acquired have different speckle appearance caused by the out of plane motion. These images can be combined to improve SNR.

3.3. Harmonic imaging

As mentioned before, ultrasound signals are distorted when traveling through the tissues. This distortion is nonlinear and as a result, harmonic components of the transmitted fundamental frequency are generated. Harmonic imaging uses those harmonics to form the image. It has been observed that the beam formed using the second harmonic is narrower and has lower side-lobes than the fundamental in homogeneous beam propagation [51,52]. Additionally, since harmonics are generated inside the body, the signal only has to pass through the fat layer once, so it is less affected by artifacts. Therefore, images generated with harmonics can potentially have better spatial and contrast resolution.

The use of harmonic components in acoustic imaging has been studied since the 1960s. Some of the first applications were in underwater acoustic imaging (sonar) and in acoustic microscopy [53]. The use of harmonics in medical ultrasound was proposed by Muir and Carstensen [54], and later on by Ward et al. [55]. Their goal was to improve lateral resolution, but those approaches were not used in commercial devices. The first ultrasound systems that used harmonic imaging were designed with the purpose of detecting harmonics generated by contrast agents. In 1994, De Jong et al. [56] studied the nonlinear movements of contrast microspheres within an acoustic field. This nonlinear behavior gives rise to harmonic components in the ultrasound backscattered signal. The bandwidth of the transducers had been previously increased to improve resolution, so it was possible to use that wide bandwidth to detect the second harmonic component. Later on, it was noticed that

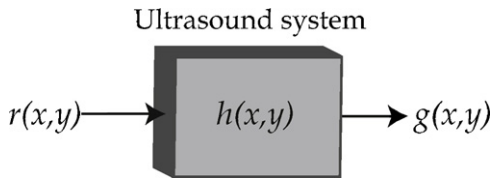

Fig. 6. The imaging system can be modeled as a linear space-variant system. The input is the spatial distribution of the structures under study and the output is the ultrasound image.

harmonics were generated by the tissues even without the use of contrast agents. At present, harmonic imaging is available in many ultrasound scanners and it is used in several fields such as breast imaging, abdominal imaging and echocardiography.

3.4. Pulse inversion

The application of harmonic imaging involves a trade-off between resolution and contrast. To increase contrast, the transmit and receive bandwidths must be narrowed, what reduces resolution. Pulse inversion is an approach that was also developed for contrast imaging, and attempts to overcome the limitations of harmonic imaging [57]. It consists on the transmission of an ultrasound beam followed by its inverted replica, and the analysis of their responses. In a linear medium, the sum of the echoes is equal to zero, but in the presence of a nonlinear medium, such as bubbles in contrast agents, the difference is related to the degree of nonlinearity. Pulse inversion can function on the entire bandwidth of the received signal, and as a result, offers improved resolution [57,58].

4. Post-processing enhancement techniques

Post-processing techniques use signal processing algorithms to improve the quality of ultrasound images after they have been generated and digitized. These techniques can reduce noise, enhance edges and improve contrast, what facilitates the interpretation of the images. Enhancement techniques can also be applied as a first step to automatic analysis, and they can make tasks such as segmentation, and quantitative measurements for characterization and identification, viable and more accurate. Segmentation and quantitative analysis techniques are not covered in this review, however, further information can be found in the following references. Thijssen [59] analyzed the speckle formation and filtering techniques, and presented basic aspects of ultrasonic tissue characterization. Noble and Boukerroui [60] did a comprehensive analysis of the techniques and applications of ultrasound image segmentation.

Ultrasound images can be modeled as the output of a linear space-variant system as seen in Fig. 6. The input $r(x, y)$ is the spatial distribution of the structures under study that is estimated by measuring the backscattered signal. The impulse response $h(x, y)$ represents the PSF of the system and the output can be written as follows:

$$g(x, y) = \int \int h(x, y; \zeta, \eta) r(\zeta, \eta)\, d\zeta\, d\eta \tag{6}$$

Due to the space variance of ultrasound, the standard convolution in two dimensions cannot be used directly to compute the output of the system, and linear space-invariant processing techniques are often not effective. Therefore, ultrasound enhancement methods usually include nonlinear, adaptive or multiscale algorithms. There are two main post-processing techniques for ultrasound images: filtering and deconvolution. The main purpose of filtering is to improve the SNR of the images. Deconvolution on the other hand, is used to improve the resolution. These techniques are explained next.

4.1. Filtering

Noise in ultrasound can be modeled as the combined effect of two components: one additive (such as electronic and thermal noise) and other multiplicative (speckle), and the statistics of speckle vary according to the scatterers distribution in the tissues. Therefore, filtering algorithms should be able to adjust to the noise properties across the image. Ultrasound filtering techniques include adaptive filters based on local statistics, anisotropic diffusion and wavelets.

4.1.1. Adaptive filters

Statistical adaptive filters are basically smoothing filters designed so that regions within the image that closely resemble the statistics of speckle are replaced by a local mean value, while regions with properties that are least similar to speckle are kept unaltered. The filter's output is computed as follows

$$f = \overline{g} + k(g - \overline{g}) \tag{7}$$

where $\overline{g}$ is the mean value within the filter window and k is the adaptive filter coefficient that is calculated based on local statistics. The first works on statistical adaptive filters to remove speckle were published in the 1980s. These filters were designed for synthetic aperture radar (SAR) images but are used for ultrasound images as well. Two of these works are the filters by Lee [61] and Frost et al. [62]. Lee used the minimum mean square error (MMSE) approach to design filters for additive noise, multiplicative noise and a combination of the two. In the case of multiplicative noise, a linear approximation was used to produce the filtering algorithm and the output was estimated based on the local mean and variance. The Frost filter uses an exponentially damped convolution kernel that adapts to the image features and is calculated based on local statistics. Other statistical adaptive filters for ultrasound images are the Bamber and Daft [63], the Dutt and Greenleaf [12], and the Chen et al. [64] filters. The first two filters use the local mean and variance to quantify the extent of speckle formation. The last one selects a region size by estimating a homogeneity value for region growth. Then, homogeneous regions are processed with an arithmetic mean filter, and edge pixels are filtered using a nonlinear median filter.

4.1.2. Anisotropic diffusion

The diffusion equation is a partial differential equation (PDE) that describes the spread of particles from regions of higher concentration to regions of lower concentration. A linear version of the diffusion equation is used to describe the distribution of heat in a region over time. In 1990, Perona and Malik [65] proposed the anisotropic diffusion as a generalization of the diffusion equation to reduce noise in images by smoothing in homogeneous regions without blurring the edges. Later on, Yongjian and Acton [66] analyzed the statistical methods for speckle suppression and Perona and Malik's anisotropic diffusion and developed the speckle reducing anisotropic diffusion method (SRAD). Yongjian and Acton noticed that Eq. (7) can be written as

$$\begin{aligned} f &= g + (1 - k)(\overline{g} - g) \\ &= g + c(\overline{g} - g) \end{aligned} \tag{8}$$

The term $(\overline{g} - g)$ can be expressed as an approximation of the Laplacian operator $div(\nabla g)$ as in the heat equation, then

$$\frac{\partial g}{\partial t} = c \cdot div(\nabla g) \tag{9}$$

Eq. (9) is the PDE that describes the isotropic diffusion phenomenon. The anisotropic diffusion equation can be obtained if c is included inside the divergence operator

$$\frac{\partial g}{\partial t} = div(c\nabla g) = c \cdot div(\nabla g) + \nabla c \cdot \nabla g \tag{10}$$

The parameter c is the diffusion coefficient. It is defined as a function of the local gradient magnitude in the image. This method provides intra-region smoothing and edge preservation in images corrupted by additive noise. The SRAD method, on the other hand, was designed to filter images corrupted by multiplicative noise. The SRAD equation can be enunciated as follows. Given an image $g_0(x, y)$ having finite power and no zero values, the output image is evolved according to the following PDE [66]

$$\begin{cases} \dfrac{\partial g(x, y; t)}{\partial t} = div(c(q)\nabla g(x, y; t)) \\ g(x, y; 0) = g_0(x, y) \end{cases} \tag{11}$$

where $c(q)$ is the diffusion coefficient and $q(x, y; t)$ is the instantaneous coefficient of variation. $q(x, y; t)$ is a function of the local gradient magnitude and Laplacian operators and acts like an edge detector. The SRAD approach applies isotropic diffusion in homogeneous regions to reduce speckle, and enhances edges by inhibiting diffusion across edges and allowing diffusion on either side of the edge. In 2007, Krissian et al. [67] proposed the oriented speckle anisotropic diffusion (OSRAD) that extends the SRAD approach to a matrix anisotropic diffusion, allowing different levels of filtering across the image contours and in the principal curvature directions.

4.1.3. Wavelets

The wavelet transform is a method that decomposes a signal into the linear combination of shifted and scaled versions of a mother wavelet. Because it is a multi-resolution approach, it provides a representation of the signal with very good time and frequency localization. Wavelets have been used in image compression, segmentation and noise reduction.

The wavelet transform of a signal $f(x)$ is given by

$$F_W(a, b) = \frac{1}{\sqrt{a}} \int_{-\infty}^{\infty} f(x)\psi\left(\frac{x-b}{a}\right) dx \tag{12}$$

where $\psi(x)$ is the mother wavelet, $a > 0$ is the scale number and b is the translation parameter. Filtering in the wavelet domain can be done by setting to zero the coefficients that correspond to noise and keeping the coefficients that contain information of the features of the image. This method is called wavelet shrinkage and uses a threshold to determine which coefficients need to be removed. There are two types of thresholding: hard and soft. Hard thresholding eliminates the coefficients that are smaller than the threshold and leaves the other ones unchanged. On the other hand, soft thresholding shrinks the remaining coefficients towards zero.

Wavelet shrinkage is effective to reduce additive noise on images. For images affected by multiplicative noise, Guo et al. [68] proposed an approach that consists in thresholding the wavelet coefficients of the logarithmically transformed image. Since logarithm is a homomorphic transform, multiplicative noise is converted into additive noise. Guo et al. used the length-4 Daubechies wavelet which provides good results in speckle suppression while preserving resolution.

Several research groups have investigated the best thresholding rule for ultrasound images. Zong et al. [69] studied hard- and soft-thresholding methods and developed a combined approach to reduce speckle and enhance image features. They used logarithmically transformed images to calculate the wavelet transform. Then, they applied soft thresholding at fine scales to remove noise, and nonlinear contrast stretching followed by hard thresholding at middle levels to preserve features and remove small noise perturbations. Gupta et al. [70] used a Bayesian formulation to find the optimum threshold for wavelet shrinkage. They based their work on the observation that the wavelet coefficients in a sub-band of logarithmically transformed images can be modeled using the generalized Gaussian distribution. The optimum threshold was estimated by minimizing the Bayes' risk function. The resultant threshold is given by the ratio of the sub-band's standard deviation to the noise's variance multiplied by a proportionality constant that depends on the size of the sub-band. Finally, a different approach was proposed by Yong et al. [71]. They developed an algorithm where speckle is iteratively filtered by the nonlinear diffusivity function on the wavelet coefficients.

4.2. Deconvolution

Deconvolution is a technique used to improve resolution in ultrasound images by counteracting the effect of the PSF. If the image is modeled as the convolution of the PSF $h(x, y)$ with the tissue reflectivity function $r(x, y)$; in frequency domain, this corresponds to the product of their Fourier transforms

$$\begin{aligned} g(x, y) &= r(x, y) * h(x, y) + \eta(x, y) \\ &= \int\int h(x-\zeta, y-\eta) r(\zeta, \eta) d\zeta d\eta + \eta(x, y) \end{aligned} \tag{13}$$

$$G(u, v) = R(u, v)H(u, v) \tag{14}$$

where u and v are the spatial frequencies, and $\eta(x, y)$ is the additive noise component. The noise term was ignored in Eq. (14) for the sake of simplicity. If the PSF is known, its effects on the image can be eliminated by dividing the spectrum of the image by the spectrum of the PSF (frequency response of the system). If the PSF is not known, it can be estimated based on the image itself. This approach is known as blind deconvolution.

The convolution model is only valid under the assumption of linear propagation and weak scattering. Linear propagation can be assumed when moderate acoustic energy is used. Weak scattering, on the other hand, can only be assumed if there are no strong specular reflectors in the tissues, as they generate artifacts [72]. Other aspects to consider are that the PSF is influenced by the tissues located between the transducer and the target, and varies across the image. Therefore, the PSF is usually estimated from the acquired RF images. To overcome the spatial variability of the PSF, it can be assumed that the PSF is shift-invariant in small segments of the image. Then, the image can be divided in segments and a PSF is estimated for each of the segments.

The reconstruction of ultrasound images by blind deconvolution often starts with the estimation of the PSF. This is typically done with a homomorphic approach using the complex cepstrum [72–76]. The cepstrum of a signal is defined as the inverse Fourier transform of the logarithm of its Fourier transform, and allows the separation of the signals $r(x, y)$ and $h(x, y)$ in the cepstrum domain.

Once the PSF is known, deconvolution can be done by multiplying the spectrum of the signal by the inverse of the frequency response of the system $H^{-1}(u, v)$. This method is rarely used, because the inversion operation can amplify noise when $H(u, v)$ is small, what results in a useless estimate. The inverse Wiener filter provides better results, and additional filters can be used to further remove noise. The Wiener equation is given by

$$R(u, v) = \frac{H^*(u, v)S_G(u, v)}{|H^2(u, v)|S_G(u, v) + N(u, v)} \tag{15}$$

where $S_G(u, v)$ and $N(u, v)$ are the power density spectra of signal $g(x, y)$ and noise respectively.

Two papers that compare the effectiveness of several filtering techniques on ultrasound images were published recently [77,78].

Loizou et al. [77] evaluated speckle reduction filters based on texture analysis, image quality metrics, and visual assessment by medical experts on ultrasound images of the carotid artery. The results show that the best filters are the first order statistics filters. Finn et al. [78] on the other hand, evaluated speckle reduction filters on echocardiographic images using simulated images and clinical videos. They compared the filters based on quality metrics and computational efficiency and concluded that the best filter is the OSRAD diffusion filter [67].

5. Conclusions

Research in ultrasound enhancement has evolved in two main branches: preprocessing techniques and post-processing algorithms. Preprocessing techniques attempt to shape the ultrasound field to compensate for signal degradations during propagation in biological tissues. They can reduce speckle and other artifacts such as shadowing and reverberations, and make the PSF more uniform across the image. Post-processing algorithms can also reduce speckle and improve the PSF. Several types of filters with different levels of complexity have been used in ultrasound images. These filters can also enhance edges and image features, and many of them can operate in real-time. However, post-processing is limited by basic physics of the image acquisition system. For example, a shadowed region cannot be restored since the data is simply not present, or the PSF may obscure fine detail beyond the ability of post-processing to retrieve it. Other aspect to consider is that post-processing may be based on preconceived notions of what certain image regions should look like, and provide inaccurate information of the imaged anatomy. Consequently, we consider that the use of preprocessing techniques should be fostered as they provide "true" improvements in SNR and resolution. Preprocessing can make certain post-processing more effective or even viable. A combined approach that includes both preprocessing and post-processing can potentially give the best results in image improvement, but it must be implemented with clear understanding of the limitations of both types of techniques.

Advances in the technology of transducers, electronics, and computers have supported the implementation of enhancement techniques and the development of the industry of ultrasound in general. For example, some preprocessing of the detected signal can be done within the probe using preamplifiers, what provides higher SNR; transducer arrays with increased number of elements can be fabricated; and in many scanners it is possible to choose among different methods for enhancement, analysis and reconstruction, that are embedded in the devices. Consequently, in the last years, the quality of the images has improved significantly, and the prices have gone down, making this technology increasingly cost-effective.

Ultrasound is becoming more quantitative as the image quality continues to improve. Speckle and other artifacts are reduced by a variety of means, and more repeatable imaging protocols are developed for specific organs and conditions. For example, metrics for fetal ultrasound have been created, with quantitative measures that are related to the extent of fetal development. However, despite of all this progress, the reduced penetration of ultrasound has restricted its use to hand-held devices and limited its applications. The penetration of ultrasound signals can be improved by reducing their frequency, and the loss in resolution could be compensated with robust enhancement and restoration techniques to perhaps go beyond the Rayleigh limit. The development of transducers that provide 360° views, and effective beamforming and compounding techniques will allow the acquisition of high quality tomographic images of the human body. These developments will extend the use of ultrasound to applications where currently CT and MRI are preferred, for example, neck and limb imaging. The advantages are to avoid patients' exposure to ionizing radiation, and the availability of high quality medical imaging at reduced cost.

References

[1] J.J. Cronan, Ultrasound: is there a future in diagnostic imaging? Journal of the American College of Radiology 3 (9) (2006) 645–646.
[2] J.F. Moreau, Re: "ultrasound: Is there a future in diagnostic imaging?", Journal of the American College of Radiology 4 (1) (2007) 78–79.
[3] P. Wells, Ultrasound imaging, Physics in Medicine and Biology 51 (13) (2006) R83–R98.
[4] C.J. Harvey, J.M. Pilcher, R.J. Eckersley, M.J. Blomley, D.O. Cosgrove, Advances in ultrasound, Clinical Radiology 57 (3) (2002) 157–177.
[5] J. Quistgaard, Signal acquisition and processing in medical diagnostic ultrasound, IEEE Signal Processing Magazine 14 (1) (1997) 67–74, cited by (since 1996) 36.
[6] A. Macovski, Medical Imaging Systems, Prentice-Hall, 1983.
[7] J. Prince, J. Links, Medical Imaging Signals and Systems, Pearson Prentice Hall, 2006.
[8] J. Ng, R. Prager, N. Kingsbury, G. Treece, A. Gee, Modeling ultrasound imaging as a linear, shift-variant system, IEEE Transactions on Ultrasonics, Ferroelectrics and Frequency Control 53 (3) (2006) 549–563.
[9] J. Goodman, Speckle Phenomena in Optics: Theory and Applications, Roberts & Co, 2007.
[10] R.F. Wagner, S.W. Smith, J.M. Sandrik, H. Lopez, Statistics of speckle in ultrasound b-scans, IEEE Transactions on Sonics and Ultrasonics 30 (3) (1983) 156–163.
[11] C.B. Burckhardt, Speckle in ultrasound b-mode scans, IEEE Transactions on Sonics and Ultrasonics 25 (1) (1978) 1–6.
[12] V. Dutt, J.F. Greenleaf, Adaptive speckle reduction filter for log-compressed b-scan images, IEEE Transactions on Medical Imaging 15 (6) (1996) 802–813.
[13] D. Kaplan, Q. Ma, On the statistical characteristics of log-compressed rayleigh signals: theoretical formulation and experimental results, Journal of the Acoustical Society of America 95 (3) (1994) 1396–1400.
[14] K.Z. Abd-Elmoniem, A.B.M. Youssef, Y.M. Kadah, Real-time speckle reduction and coherence enhancement in ultrasound imaging via nonlinear anisotropic diffusion, IEEE Transactions on Biomedical Engineering 49 (9) (2002) 997–1014.
[15] F.W. Kremkau, K.J.W. Taylor, Artifacts in ultrasound imaging, Journal of Ultrasound in Medicine 5 (4) (1986) 227–237.
[16] K.S.B.M. Feldman, Us artifacts, Radiographics 29 (4) (2009) 1179–1189.
[17] F. Laing, A. Kurtz, The importance of ultrasonic side-lobe artifacts, Radiology 145 (3) (1982) 763–768.
[18] J.-Y. Lu, H. Zou, J.F. Greenleaf, Biomedical ultrasound beam forming, Ultrasound in Medicine and Biology 20 (5) (1994) 403–428.
[19] J.A. Jensen, S.I. Nikolov, K.L. Gammelmark, M.H. Pedersen, Synthetic aperture ultrasound imaging, Ultrasonics 44, Suppl. (0) (2006) e5–e15, in: Proceedings of Ultrasonics International (UI05) and World Congress on Ultrasonics (WCU). doi:10.1016/j.ultras.2006.07.017. http://www.sciencedirect.com/science/article/pii/S0041624X06003374.
[20] S.G. Mandersson, Bengt, Weighted least-squares pulse-shaping filters with application to ultrasonic signals, IEEE Transactions on Ultrasonics, Ferroelectrics, and Frequency Control 36 (1) (1989) 109–113, cited by (since 1996) 5.
[21] W. Wilkening, B. Brendel, H. Jiang, J. Lazenby, H. Ermert, Optimized receive filters and phase-coded pulse sequences for contrast agent and nonlinear imaging 2, Ultrasonics Symposium, 2001 IEEE, pp. 1733–1737, cited by (since 1996) 10.
[22] D.A. Guenther, W.F. Walker, Optimal apodization design for medical ultrasound using constrained least squares. Part i: theory, IEEE Transactions on Ultrasonics, Ferroelectrics, and Frequency Control 54 (2) (2007) 332–341.
[23] T. Misaridis, J. Jensen, Use of modulated excitation signals in medical ultrasound. Part i: basic concepts and expected benefits, IEEE Transactions on Ultrasonics, Ferroelectrics and Frequency Control 52 (2) (2005) 177–191, doi:10.1109/TUFFC.2005.1406545.
[24] T. Misaridis, J. Jensen, Use of modulated excitation signals in medical ultrasound. Part ii: design and performance for medical imaging applications, IEEE Transactions on Ultrasonics, Ferroelectrics and Frequency Control 52 (2) (2005) 192–207, doi:10.1109/TUFFC.2005.1406546.
[25] T. Misaridis, J. Jensen, Use of modulated excitation signals in medical ultrasound. Part iii: high frame rate imaging, IEEE Transactions on Ultrasonics, Ferroelectrics and Frequency Control 52 (2) (2005) 208–219, doi:10.1109/TUFFC.2005.1406547.
[26] H.X. Chiao, Coded excitation for diagnostic ultrasound: A system developer's perspective, IEEE Transactions on Ultrasonics, Ferroelectrics, and Frequency Control 52 (2) (2005) 160–170, cited by (since 1996) 113.
[27] J.A. Jensen, Field: a program for simulating ultrasound systems, Medical and Biological Engineering and Computing 34 (Suppl. (1)) (1996) 351–352.
[28] J.A. Jensen, N.B. Svendsen, Calculation of pressure fields from arbitrarily shaped, apodized, and excited ultrasound transducers, IEEE Transactions on Ultrasonics, Ferroelectrics, and Frequency Control 39 (2) (1992) 262–267.
[29] S.H. Contreras Ortiz, J.J. Macione, M.D. Fox, Enhancement of ultrasound images by displacement, averaging, and interlacing, Journal of Electronic Imaging 19 (1) (2010).

[30] P.M. Shankar, V.L. Newhouse, Speckle reduction with improved resolution in ultrasound images, IEEE Transactions on Sonics and Ultrasonics 32 (4) (1985) 537–543.
[31] P.M. Shankar, Speckle reduction in ultrasound b-scans using weighted averaging in spatial compounding, IEEE Transactions on Ultrasonics Ferroelectrics, and Frequency Control UFFC-33 (6) (1986) 754–758.
[32] G.R. Bashford, J.L. Morse, Circular ultrasound compounding by designed matrix weighting, IEEE Transactions on Medical Imaging 25 (6) (2006) 732–741.
[33] M. Berson, A. Roncin, L. Pourcelot, Compound scanning with an electrically steered beam, Ultrasonic Imaging 3 (3) (1981) 303–308.
[34] S.K. Jespersen, J.E. Wilhjelm, H. Sillesen, Multi-angle compound imaging, Ultrasonic Imaging 20 (2) (1998) 81–102.
[35] G.E. Trahey, S.W. Smith, O.T. von Ramm, Speckle pattern correlation with lateral aperture translation: experimental results and implications for spatial compounding, Modelling, Measurement and Control A UFFC-33 (3) (1986) 257–264.
[36] M. Vogt, H. Ermert, Limited-angle spatial compound imaging of skin with high-frequency ultrasound (20 mhz), IEEE Transactions on Ultrasonics, Ferroelectrics, and Frequency Control 55 (9) (2008) 1975–1983.
[37] C. Hansen, N. Huttebrauker, W. Wilkening, S. Brunke, H. Ermert, Full angle spatial compounding for improved replenishment analyses in contrast perfusion imaging: In vitro studies, IEEE Transactions on Ultrasonics, Ferroelectrics, and Frequency Control 55 (4) (2008) 819–830.
[38] J. Macione, Z. Yang, M. Fox, Paired-angle multiplicative compounding, Ultrasonic Imaging 30 (2) (2008) 112–130.
[39] L. Pai Chi, M. O'Donnell, Elevational spatial compounding, Ultrasonic Imaging 16 (3) (1994) 176–189.
[40] V. Behar, D. Adam, Z. Friedman, A new method of spatial compounding imaging, Ultrasonics 41 (5) (2003) 377–384.
[41] D. Adam, S. Beilin-Nissan, Z. Friedman, V. Behar, The combined effect of spatial compounding and nonlinear filtering on the speckle reduction in ultrasound images, Ultrasonics 44 (2) (2006) 166–181.
[42] J.E. Wilhjelm, M.S. Jensen, S.K. Jespersen, B. Sahl, E. Falk, Visual and quantitative evaluation of selected image combination schemes in ultrasound spatial compound scanning, IEEE Transactions on Medical Imaging 23 (2) (2004) 181–190.
[43] J.G. Abbott, F.L. Thurstone, Acoustic speckle: Theory and experimental analysis, Ultrasonic Imaging 1 (4) (1979) 303–324.
[44] G.E. Trahey, J.W. Allison, S.W. Smith, O.T. Von Ramm, A quantitative approach to speckle reduction via frequency compounding, Ultrasonic Imaging 8 (3) (1986) 151–164.
[45] P.A. Magnin, O.T. von Ramm, F.L. Thurstone, Frequency compounding for speckle contrast reduction in phased array images, Ultrasonic Imaging 4 (3) (1982) 267–281.
[46] J.H. Chang, H.H. Kim, J. Lee, K.K. Shung, Frequency compounded imaging with a high-frequency dual element transducer, Ultrasonics 50 (4-5) (2010) 453–457.
[47] V.L. Newhouse, N.M. Bilgutay, J. Saniie, E.S. Furgason, Flaw-to-grain echo enhancement by split-spectrum processing, Ultrasonics 20 (2) (1982) 59–68.
[48] R.G. Dantas, E.T. Costa, Ultrasound speckle reduction using modified gabor filters, IEEE Transactions on Ultrasonics, Ferroelectrics, and Frequency Control 54 (3) (2007) 530–538.
[49] J.R. Sanchez, M. Oelze, M.L. Oelze, An ultrasonic imaging speckle-suppression and contrast-enhancement technique by means of frequency compounding and coded excitation, IEEE Transactions on Ultrasonics, Ferroelectrics, and Frequency Control 56 (7) (2009) 1327–1339.
[50] P.C. Li, M.J. Chen, Strain compounding: a new approach for speckle reduction, IEEE Transactions on Ultrasonics, Ferroelectrics, and Frequency Control 49 (1) (2002) 39–46.
[51] T. Christopher, Finite amplitude distortion-based inhomogeneous pulse echo ultrasonic imaging, IEEE Transactions on Ultrasonics, Ferroelectrics, and Frequency Control 44 (1) (1997) 125–139.
[52] V.F. Humphrey, Nonlinear propagation in ultrasonic fields: measurements, modelling and harmonic imaging, Ultrasonics 38 (1) (2000) 267–272.
[53] F.A. Duck, Nonlinear acoustics in diagnostic ultrasound, Ultrasound in Medicine and Biology 28 (1) (2002) 1–18.
[54] T.G. Muir, E.L. Carstensen, Prediction of nonlinear acoustic effects at biomedical frequencies and intensities, Ultrasound in Medicine and Biology 6 (4) (1980) 345–357.
[55] B. Ward, A.C. Baker, V.F. Humphrey, Nonlinear propagation applied to the improvement of resolution in diagnostic medical ultrasound, Journal of the Acoustical Society of America 101 (1) (1997) 143–154.
[56] N. De Jong, R. Cornet, C.T. Lancee, Higher harmonics of vibrating gas-filled microspheres. part two: Measurements, Ultrasonics 32 (6) (1994) 455–459.
[57] D.H. Simpson, C.T. Chin, P.N. Burns, Pulse inversion doppler: a new method for detecting nonlinear echoes from microbubble contrast agents, IEEE Transactions on Ultrasonics, Ferroelectrics, and Frequency Control 46 (2) (1999) 372–382.
[58] P.J.A. Frinking, A. Bouakaz, J. Kirkhorn, F.J. Ten Cate, N. de Jong, Ultrasound contrast imaging: current and new potential methods, Ultrasound in Medicine and Biology 26 (6) (2000) 965–975.
[59] J. Thijssen, Ultrasonic speckle formation, analysis and processing applied to tissue characterization, Pattern Recognition Letters 24 (4–5) (2003) 659–675.
[60] J. Noble, D. Boukerroui, Ultrasound image segmentation: a survey, IEEE Transactions on Medical Imaging 25 (8) (2006) 987–1010.
[61] J.-S. Lee, Digital image enhancement and noise filtering by use of local statistics, IEEE Transactions on Pattern Analysis and Machine Intelligence PAMI 2 (2) (1980) 165–168.
[62] V.S. Frost, J.A. Stiles, K.S. Shanmugan, J.C. Holtzman, A model for radar images and its application to adaptive digital filtering of multiplicative noise, IEEE Transactions on Pattern Analysis and Machine Intelligence PAMI 4 (2) (1982) 157–166.
[63] J.C. Bamber, C. Daft, Adaptive filtering for reduction of speckle in ultrasonic pulse-echo images, Ultrasonics 24 (1) (1986) 41–44.
[64] Y. Chen, R. Yin, P. Flynn, S. Broschat, Aggressive region growing for speckle reduction in ultrasound images, Pattern Recognition Letters 24 (4–5) (2003) 677–691.
[65] P. Perona, J. Malik, Scale-space and edge detection using anisotropic diffusion, IEEE Transactions on Pattern Analysis and Machine Intelligence 12 (7) (1990) 629–639.
[66] Y. Yongjian, S.T. Acton, Speckle reducing anisotropic diffusion, IEEE Transactions on Image Processing 11 (11) (2002) 1260–1270.
[67] K. Krissian, C.F. Westin, R. Kikinis, K.G. Vosburgh, Oriented speckle reducing anisotropic diffusion, IEEE Transactions on Image Processing 16 (5) (2007) 1412–1424.
[68] H. Guo, J.E. Odegard, M. Lang, R.A. Gopinath, I.W. Selesnick, C.S. Burrus, Wavelet based speckle reduction with application to sar based atd/r, in: in: Proceedings of the ICIP-94, IEEE International Conference on Image Processing, Vol. 1, 1994, pp. 75–79.
[69] X. Zong, A.F. Laine, E.A. Geiser, Speckle reduction and contrast enhancement of echocardiograms via multiscale nonlinear processing, IEEE Transactions on Medical Imaging 17 (4) (1998) 532–540.
[70] S. Gupta, R. Chauhan, S. Sexana, Wavelet-based statistical approach for speckle reduction in medical ultrasound images, Medical and Biological Engineering and Computing 42 (2) (2004) 189–192.
[71] Y. Yong, M.M. Croitoru, A. Bidani, J.B. Zwischenberger, J.J.W. Clark, Nonlinear multiscale wavelet diffusion for speckle suppression and edge enhancement in ultrasound images, IEEE Transactions on Medical Imaging 25 (3) (2006) 297–311.
[72] O.V. Michailovich, D. Adam, A novel approach to the 2-d blind deconvolution problem in medical ultrasound, IEEE Transactions on Medical Imaging 24 (1) (2005) 86–104.
[73] U.R. Abeyratne, A.P. Petropulu, J.M. Reid, Higher order spectra based deconvolution of ultrasound images, IEEE Transactions on Ultrasonics, Ferroelectrics, and Frequency Control 42 (6) (1995) 1064–1075.
[74] T. Taxt, Comparison of cepstrum-based methods for radial blind deconvolution of ultrasound images, IEEE Transactions on Ultrasonics, Ferroelectrics, and Frequency Control 44 (3) (1997) 666–674.
[75] T. Taxt, J. Strand, Two-dimensional noise-robust blind deconvolution of ultrasound images, IEEE Transactions on Ultrasonics, Ferroelectrics, and Frequency Control 48 (4) (2001) 861–867.
[76] S. Wan, B.I. Raju, M.A. Srinivasan, Robust deconvolution of high-frequency ultrasound images using higher-order spectral analysis and wavelets, IEEE Transactions on Ultrasonics, Ferroelectrics, and Frequency Control 50 (10) (2003) 1286–1295.
[77] C.P. Loizou, C.S. Pattichis, C.I. Christodoulou, R.S.H. Istepanian, M. Pantziaris, A. Nicolaides, Comparative evaluation of despeckle filtering in ultrasound imaging of the carotid artery, IEEE Transactions on Ultrasonics, Ferroelectrics and Frequency Control 52 (10) (2005) 1653–1669.
[78] S. Finn, M. Glavin, E. Jones, Echocardiographic speckle reduction comparison, IEEE Transactions on Ultrasonics, Ferroelectrics and Frequency Control 58 (1) (2011) 82–101.